Published online 10 January 2008 *Nucleic Acids Research, 2008, Vol. 36, No. 4* ***1369–1379***
doi:10.1093/nar/gkm1169

EXOG, a novel paralog of Endonuclease G in higher eukaryotes

Iwona A. Cymerman[1], Inn Chung[2], Benedikt M. Beckmann[2], Janusz M. Bujnicki[1,3] and Gregor Meiss[2,*]

[1]Laboratory of Bioinformatics and Protein Engineering, International Institute of Molecular and Cell Biology, Trojdena 4, 02-109 Warsaw, Poland, [2]Institute of Biochemistry, Faculty of Biology and Chemistry, Justus-Liebig-University Giessen, Heinrich-Buff-Ring 58, D-35392 Giessen, Germany and [3]Institute of Molecular Biology and Biotechnology, Faculty of Biology, Adam Mickiewicz University, Umultowska 89, 61-614 Poznan, Poland.

Received November 1, 2007; Revised and Accepted December 19, 2007

ABSTRACT

Evolutionary conserved mitochondrial nucleases are involved in programmed cell death and normal cell proliferation in lower and higher eukaryotes. The endo/exonuclease Nuc1p, also termed 'yeast Endonuclease G (EndoG)', is a member of this class of enzymes that differs from mammalian homologs by the presence of a 5′–3′ exonuclease activity in addition to its broad spectrum endonuclease activity. However, this exonuclease activity is thought to be essential for a function of the yeast enzyme in DNA recombination and repair. Here we show that higher eukaryotes in addition to EndoG contain its paralog 'EXOG', a novel EndoG-like mitochondrial endo/exonuclease. We find that during metazoan evolution duplication of an ancestral nuclease gene obviously generated the paralogous EndoG- and EXOG-protein subfamilies in higher eukaryotes, thereby maintaining the full endo/exonuclease activity found in mitochondria of lower eukaryotes. We demonstrate that human EXOG is a dimeric mitochondrial enzyme that displays 5′–3′ exonuclease activity and further differs from EndoG in substrate specificity. We hypothesize that in higher eukaryotes the complementary enzymatic activities of EndoG and EXOG probably together account for both, the lethal and vital functions of conserved mitochondrial endo/exonucleases.

INTRODUCTION

Mitochondria contain at least one highly conserved sugar-non-specific nuclease that contributes to vital and lethal functions in eukaryotes (1–3). One of the functionally best studied representatives of these mitochondrial enzymes from lower eukaryotes is the endo/exonuclease Nuc1p from budding yeast (4,5). Several investigations have clearly defined that besides to a lethal role during cell death Nuc1p is also required for normal cell proliferation and similar functions have been reported for its *Caenorhabditis elegans* and mammalian homologs, CPS-6 and Endonuclease G (EndoG), respectively (6–11).

Whereas during programmed cell death yeast Nuc1p and *C. elegans* EndoG are activated in a caspase-independent manner, the role of mammalian EndoG in apoptosis apparently is of much higher complexity, as experimental results concerning its recruitment have disclosed a partially controversial situation (9,12–14). Moreover, the finding that a knock out of EndoG in mice apparently does not lead to any obvious abnormality in this organism has been quite perplexing and caused scepticism regarding a vital function of this endonuclease in mammals (15–17).

To carry out its dual role in cell death and normal cell proliferation Nuc1p is endowed with two different enzymatic activities. Besides having a broad spectrum endonuclease activity towards DNA and RNA the enzyme also exerts 5′–3′ exonuclease activity enabling it to induce single stranded gaps into double stranded DNA in the course of DNA recombination and repair events (4). Interestingly, this exonuclease activity is not found in known mammalian EndoG family members, which are pure endonucleases (7,18–21).

The controversial results concerning the cellular role of mammalian EndoG and its lack of 5′–3′ exonuclease activity prompted us to search for similar enzymes that might back up or complement EndoG function in mammals. Interestingly, we found paralogous genes in higher eukaryotes, previously termed *endonuclease G-like-1*, that obviously result from duplication of an ancestral endo/exonuclease gene (Figure 1). Though the human

*To whom correspondence should be addressed. Tel: +49 641 99 35410; Fax: +49 641 99 35409; Email: gf45@uni-giessen.de

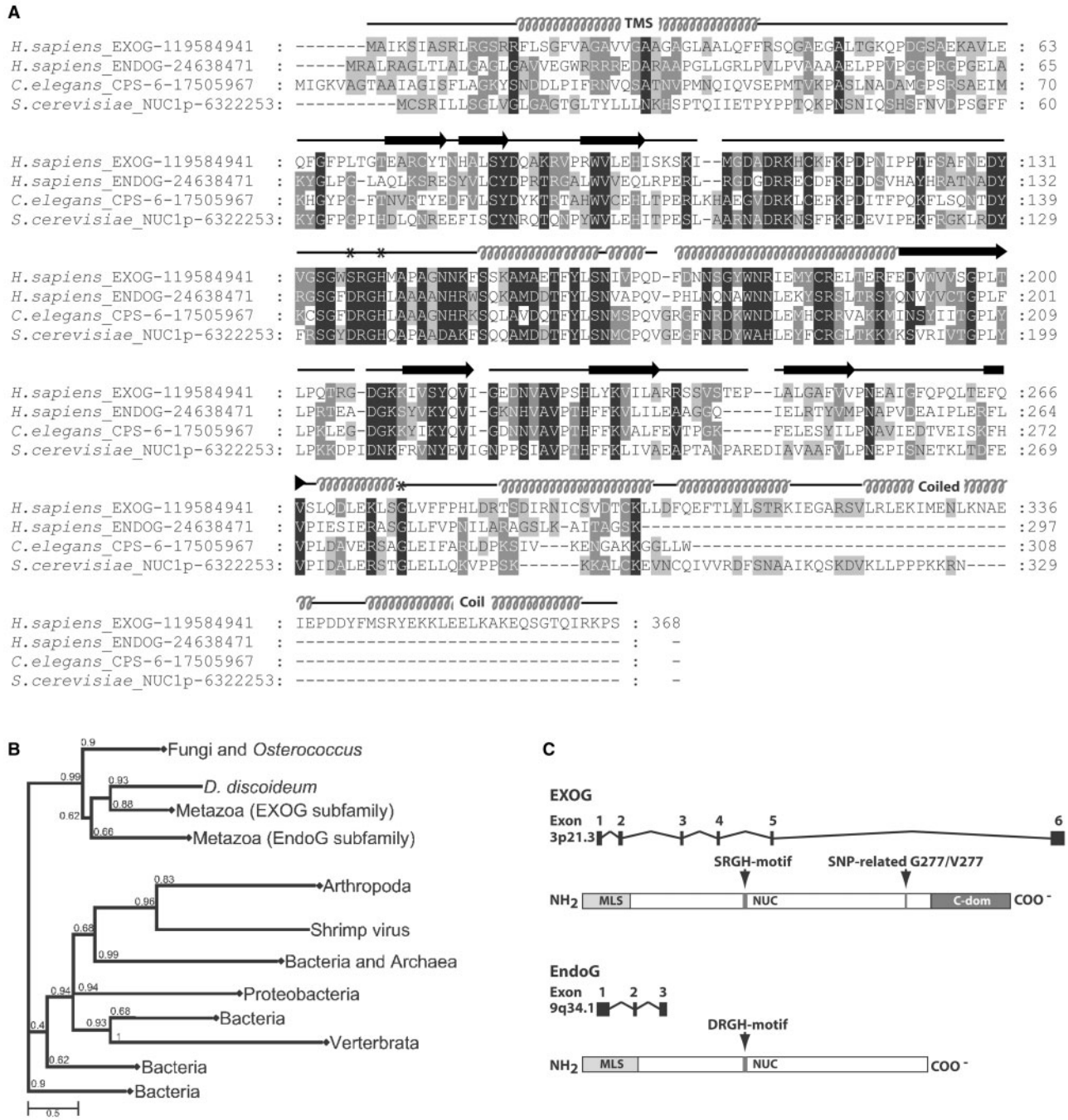

Figure 1. Sequence and evolutionary analysis of EndoG and EXOG. (**A**) Alignment of human EXOG and EndoG protein sequences with homologous proteins from *C. elegans* and yeast. Human EXOG contains a predicted helical transmembrane segment (TMS, residues 16–38) within the leader sequence (residues 1–41) and a predicted C-terminal coiled coil domain as indicated above the sequences. The asterisks denote the amino acid residues Ser137, His140 and Gly277 of EXOG exchanged in this study. β-strands are shown as arrows and helices as spiral lines. (**B**) Phylogenetic maximum likelihood (ML) tree of EXOG protein and its homologs. The branches containing more than one sequence were compressed and are indicated by a square. Note, branches of the tree are named according to the taxa of organisms encoding the sugar non-specific nucleases. Values at the nodes indicate the statistical support for the particular clades calculated according to aLRT test. (**C**) Genomic structure and domain organization of EXOG and EndoG. The human EXOG gene locates to chromosome 3 (3p21.3) and contains six exons spanning a genomic region of 28.35 kb. EXOG is a protein of 368 amino acid residues, corresponding to a theoretical mass of 41.1 kDa. The human EndoG gene is located on chromomsome 9 (9q34.1) and contains three exons spanning 4.15 kb. Human EndoG is a protein of 297 amino acid residues corresponding to a calculated mass of 32.6 kDa.

endonuclease G-like-1 gene has been described twice previously, demonstrating ubiquitous expression on the mRNA level in all tissues tested, it has not been shown yet whether it encodes a functional enzyme and what the properties and functions of this enzyme would be (22,23). Here we show that the gene product of *endonuclease G-like-1* is a mitochondrial endo/exonuclease displaying both, endonuclease and 5′–3′ exonuclease activity. Due to

its complementary enzymatic activities and a common evolutionary origin with EndoG we termed this novel endo/exonuclease 'EXOG'. Intriguingly, together EndoG and EXOG unite all enzymatic activities found in fungal single protein endo/exonucleases, suggesting that in higher eukaryotes the major mitochondrial nuclease activity and hence its vital and lethal cellular functions are probably distributed over these two enzymes.

MATERIALS AND METHODS

Bioinformatic analyses

Sequence alignments, selection of evolutionary models and phylogenetic reconstructions by the maximum likelihood (ML) method were performed using PROMALS (24), PROTTEST (25), and PHYML (26,27) followed by aLRT tests (28). Secondary structure and transmembrane region predictions were carried out via the GeneSilico meta-server gateway (29) and according to program DSSP (30).

Cell culture, transfection and immunoprecipitation

MCF-7, HeLa and HEK-293 cells cultured according to standard conditions were used in transfection experiments using TransFast or PolyFect reagents. EXOG (*Endonuclease G-like-1*) cDNA was obtained from Invitrogen (ULTIMATEHORF CLONE ID: IOH41653). For transient expression EXOG and EndoG cDNAs (31) were amplified by PCR and inserted into p3×-FLAG-CMV-14, EXOG cDNA also into pEGFP-N1 and pEGFP-C1. Immunoprecipitation of 3 × FLAG-tagged proteins was achieved using EZview™ Red ANTI-FLAG® M2 Affinity Gel. Where intended, apoptosis was induced 24 h post transfection using staurosporine at a final concentration of 3 μM and cells were fixed after 3 h of incubation.

Mitochondrial subfractionation

Mitochondria were isolated with the Qproteome Mitochondria Isolation Kit. Immediately after isolation mitochondria were sonicated and then centrifuged at 90 000 r.p.m. for 50 min at 4°C (Beckman Coulter, Optima Max Ultracentrifuge), resulting in the mitochondrial membrane (pellet) and soluble fractions (supernatant), respectively. Western blotting was conducted using following antibodies: anti-cytochrome *c*; anti-FLAG M2; anti-COXIV; anti-TOM20, and IgG anti-mouse secondary antibody. Chemiluminescent detection was performed using an ECL kit according to the manufacturer's protocol.

Immunostaining and confocal microscopy

For immunostaining cells on cover slips were fixed with ice-cold 4% paraformaldehyde/PBS, washed with PBS and incubated with primary antibodies (rabbit anti-GFP; mouse anti cytochrome c) diluted 1:500 in blocking solution (10% horse serum, 2% BSA, 4% sucrose and 0.1% Triton X-100 in PBS) at 4°C overnight. After washing in PBS cells were treated with secondary antibodies (anti rabbit IgG-Alexa488; anti mouse IgG-Alexa594) diluted 1:500 as above for 1.5 h at RT. A LEICA TCS SP2 AOBS microscope was used for confocal imaging. DAPI and pDsRed2-Mito (40) were used as nuclear and mitochondrial staining markers, respectively.

Post embedded immunogold cytochemistry and electron microscopy

Osmium-free embedding and immunolabeling were performed according to protocols published previously (32). Ultrathin sections were subjected to immunoreactions with a primary rabbit anti-GFP antibody (Abcam, ab290-50) diluted 1:50 in TBST (50 mM Tris buffer, pH 7.4, 0.6% NaCl and 0.1% Triton) and secondary anti rabbit IgG antibody (Merck MOPA-31565) coupled to 5 nm gold particles (dilution 1: 25 in TBST). Electron microscopy images were captured using a Jeol 1200 EX transmission electron microscope operating at 80 kV.

Recombinant protein production and site-directed mutagenesis

Recombinant EXOG was expressed in *Escherichia coli* BL21Star(DE3) cells using the pET160/GW/D-TOPO vector and purified by Ni^{2+}-NTA-affinity chromatography under denaturing conditions. Renaturation was performed according to the iFOLD2 system (Novagen) by flash dilution into a buffer consisting of 50 mM HEPES pH 7.5, 1.5 M sorbitol, 1 mM TCEP; 24 mM NaCl and 1 mM KCl. The concentration of unfolded and refolded recombinant EXOG was determined spectrophotometrically at 280 nm using a molar extinction coefficient of $\varepsilon = 40480$. The purity of EXOG variants was determined by SDS-PAGE. Site-directed mutagenesis was done using PCR as described previously (33).

Discontinuous native PAGE (BN-PAGE)

To assess the oligomeric state of EXOG, a protocol for a discontinuous native polyacrylamide gel electrophoresis was followed, known as 'blue native' or 'BN-PAGE', using a 5–35% native polyacrylamide gradient gel under non-reducing conditions and the dye Blue G (Serva), as described earlier in detail (34,35).

Enzymatic activity assays

Enzymatic assays with supercoiled, open circular and circular single stranded DNA from phage ΦX174 were done in 50 mM Tris pH 7.0, supplemented with 2.5 mM $MgCl_2$ and $MnCl_2$, each. If not stated otherwise a typical cleavage reaction was performed with a final concentration of 240 nM refolded, recombinant EXOG and 70 ng/μl DNA. Cleavage products were separated by agarose gel electrophoresis and the program ImageJ (http://rsb.info.nih.gov/ij/) was used to quantify individual bands from ethidium bromide stained gels. In order to determine relative cleavage rates the decrease in concentration of the individual substrates (supercoiled, open circular or circular single stranded DNA, respectively) was measured and the initial amount of substrate was set at 1 or 100%.

The cleavage of radioactively labeled oligonucleotides was analyzed by denaturing polyacrylamide gel electrophoresis as well as thin layer anion-exchange chromatography under denaturing conditions. Denaturing polyacrylamide gel electrophoresis was performed using 25% polyacrylamide gels containing 7 M urea in 1 × TBE-buffer. Thin layer chromatography was performed using a lysate of total yeast RNA in 7 M urea as the eluens. To assess the polarity of the exonuclease activity of EXOG, the 27- and 12-mer oligonucleotides (EXOUP 5′-CCAA GATATCAGGCGCCAGATCTTCCC-3′ and EXOUP-5′ 5′-CCAAGATATCAG-3′) were radioactively labelled either at their 5′-ends with [γ^{32}P]-ATP and polynucleotidekinase or, at their 3′-ends with [α^{32}P]-ddATP and terminal desoxynucleotidyl transferase. Double stranded oligonucleotide substrates were produced by annealing of the unlabeled complementary strand. The exonucleases $RecJ_f$ and ExoI were used to digest the labeled oligonucleotides according to the recommendation of the supplier (NEB), leading to the production of mononucleotides ($RecJ_f$) and dinucleotides (ExoI) used as size markers. After the separation of cleavage products by electrophoresis or on DEAE-cellulose thin layer plates at 65°C, data were collected by autoradiography.

RESULTS

Phylogenetic analysis of EndoG paralogs

With the aim to identify enzymes that might back up or complement EndoG function in mammals, sequence searches with PSI-BLAST (36,37) and bovine EndoG as the query, were performed, that resulted in the identification of a total of 562 similar protein sequences. Alignments of these protein sequences revealed the presence of a distinct family of sugar non-specific nucleases in higher eukaryotes each encoded on a different chromosome than their paralogous EndoG counterparts. On the primary sequence level these paralogs can be clearly distinguished from the previously known EndoG-family members by the presence of an 'SRGH' catalytic motif instead of 'DRGH' and an additional C-terminal domain of approximately 70 amino acid residues length (Figure 1A and Supplementary Figure S1). In order to trace the evolutionary origin of these EndoG paralogs, 168 representative protein sequences were chosen for the construction of an evolutionary tree (Figure 1B). Among higher eukaryotes the tree reveals two branches of sugar non-specifc nucleases corresponding to orthologs of the previously studied EndoG-proteins and orthologs of the newly discovered EndoG-paralogs, which both are present e.g. in *Xenopus laevis* and *Homo sapiens* (see Supplementary Figures S1 and S2). The tree suggests that a duplication of an ancestral endo/exonuclease gene leading to these nuclease subfamilies occurred after the separation of animalia and fungal lineages and at the latest in the common ancestors of deuterostomes. A more detailed subtree of EndoG- and EXOG-protein subfamilies is given in Supplementary Figure S2. In humans, a paralog—we named 'EXOG'—was found which is encoded by a gene previously named '*endonuclease G-like-1*'. This gene is located on chromosome 3, whereas the human EndoG-gene locates to chromosome 9 (Figure 1C) (21).

Given the differences in sequence composition and domain organization between EndoG and its paralog EXOG we next wanted to find out whether EXOG is a functional enzyme, where the enzyme is located in the cell and what the enzymatic properties of this enzyme would be.

Endonuclease G-like-1 encodes a functional enzyme

In order to test whether *endonuclease G-like-1* encodes an active enzyme, we expressed 3 × FLAG fusion proteins of human EXOG, and, for comparison, of bovine EndoG in mammalian cell lines. Confocal imaging of transfected HeLa cells employing antibodies against the 3 × FLAG-tag revealed that EXOG, similarly to EndoG, localizes to mitochondria (Figure 2A, left panel). To detect a putative endonuclease activity of mitochondrial EXOG we purified EXOG and EndoG from transiently transfected HEK 293-cells by immunoprecipitation and performed cleavage assays using various circular DNA substrates (supercoiled, open circular, and circular single stranded DNA from phage ΦX174). Of note, though being expressed in parallel from similar constructs, an approximately 25 times higher yield of immunoreactive EndoG compared to EXOG was obtained from the immunoprecipitation experiments. For the DNA cleavage assays, therefore, concentrations were adjusted and the same amount of immunoreactive material from EXOG and EndoG preparations was used (Figure 2A, right panel). In contrast to EndoG, which cleaved all three substrates with nearly identical rates, EXOG only cleaved circular single stranded DNA efficiently (Figure 2B). This demonstrates that EXOG indeed is a functional mitochondrial enzyme displaying endonuclease activity preferentially, but not exclusively (see below), on single stranded DNA and that EndoG and EXOG clearly differ in their substrate specificities. The question whether EXOG also displays exonuclease activity, as demonstrated earlier for yeast Nuc1p (4,7), had to be assessed by the cleavage of radioactively labeled oligonucleotide substrates as described below, since such an activity can hardly be seen from cleavage experiments using circular DNA molecules.

EXOG locates to the inner mitochondrial membrane

In order to characterize the subcellular localization of EXOG in more detail we investigated the localization of transiently expressed fusion proteins of EXOG with EGFP by mitochondrial subfractionation, immunogold staining and confocal laser scanning microscopy (Figure 3). Following mitochondrial subfractionation EXOG and EndoG were both found in membrane fractions, co-localizing with CYT*C*, COX-IV and TOM20 (Figure 3A). These proteins reside in the intermembrane space (IMS) and inner (IMM) or outer (OMM) mitochondrial membranes, respectively, strongly pointing towards a membrane association (IMM or OMM) of EXOG. However, in electron micrographs of immunogold stained samples of mitochondria from

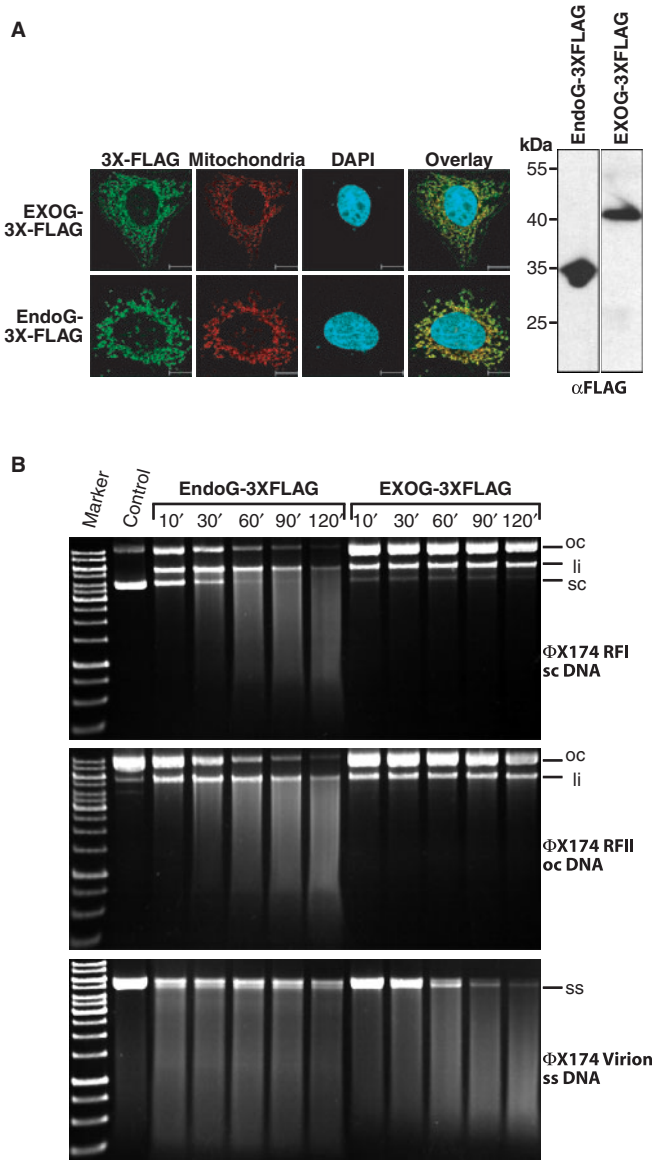

Figure 2. EXOG is a functional enzyme preferring single stranded DNA. (**A**) Confocal imaging and immunoblotting of 3 × FLAG-tagged human EXOG and bovine EndoG. Both proteins localize to mitochondria as visualized by confocal imaging using antibody against the 3 × FLAG-tag and pDsRed2-Mito as a mitochondrial marker (left panel). The proteins run on SDS-PAGE as visualized by western blotting (right panel) with the expected sizes of 30.4 kDa (EndoG) and 40 kDa (EXOG). (**B**) Immunoprecipitated EXOG displays strong nicking activity towards supercoiled DNA (ΦX174 RFI) and prefers cleavage of circular single stranded DNA (ΦX174 Virion). In contrast, bovine EndoG cleaves all substrates with nearly identical rates.

transfected cells expressing EXOG, the protein was very often found delineating the cristae, thereby revealing an association of EXOG with the inner mitochondrial membrane (Figure 3B), similarly as found for the yeast homolog Nuc1p and mammalian EndoG (1,8).

An N-terminal hydrophobic transmembrane segment accounts for mitochondrial uptake of EXOG

To define the region responsible for association of EXOG with the inner mitochondrial membrane we reanalyzed the

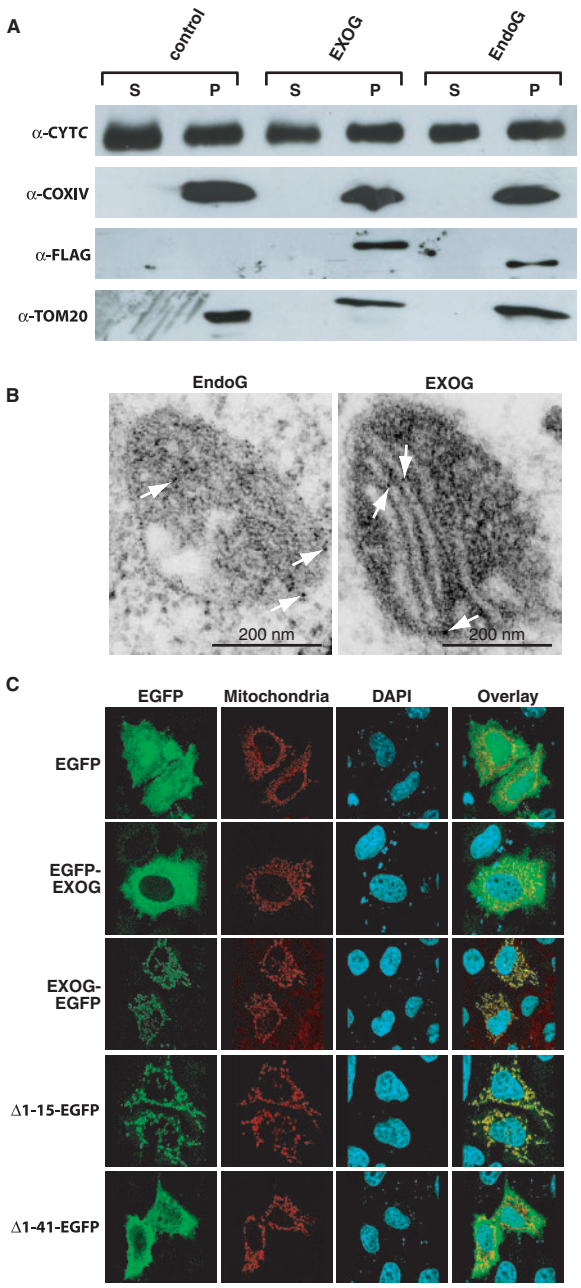

Figure 3. Submitochondrial localization of EXOG. (**A**) Mitochondrial subfractionation of cells expressing 3 × -FLAG tagged EndoG and EXOG reveal the localization of the proteins in membrane fractions (P, pellet) and exclude their presence as soluble proteins of the intermembrane space or the mitochondrial matrix (S, supernatant). (**B**) Electronmicrographs showing ultrathin sections of cells transfected with C-terminally EGFP-tagged EXOG and EndoG. Both proteins are often found delineating the cristae, pointing towards an association with the inner mitochondrial membrane. White arrows exemplary indicate positive signals from immunogold stained particles. (**C**) Requirement of the predicted transmembrane helix for mitochondrial uptake of EXOG. Blocking of the MLS by N-terminal fusion of EGFP (EGFP-EXOG) to EXOG abrogates mitochondrial uptake of EXOG, whereas fusion of EGFP to the C-terminus (EXOG-EGFP) allows monitoring the mitochondrial localization of the enzyme. The first 15 amino acid residues of the MLS are dispensable for mitochondrial uptake of EXOG (Δ1-15-EXOG-EGFP), whereas amino acid residues 16–41 comprising the putative helical transmembrane segment (Δ1-41-EXOG-EGFP) are required for mitochondrial localization of EXOG.

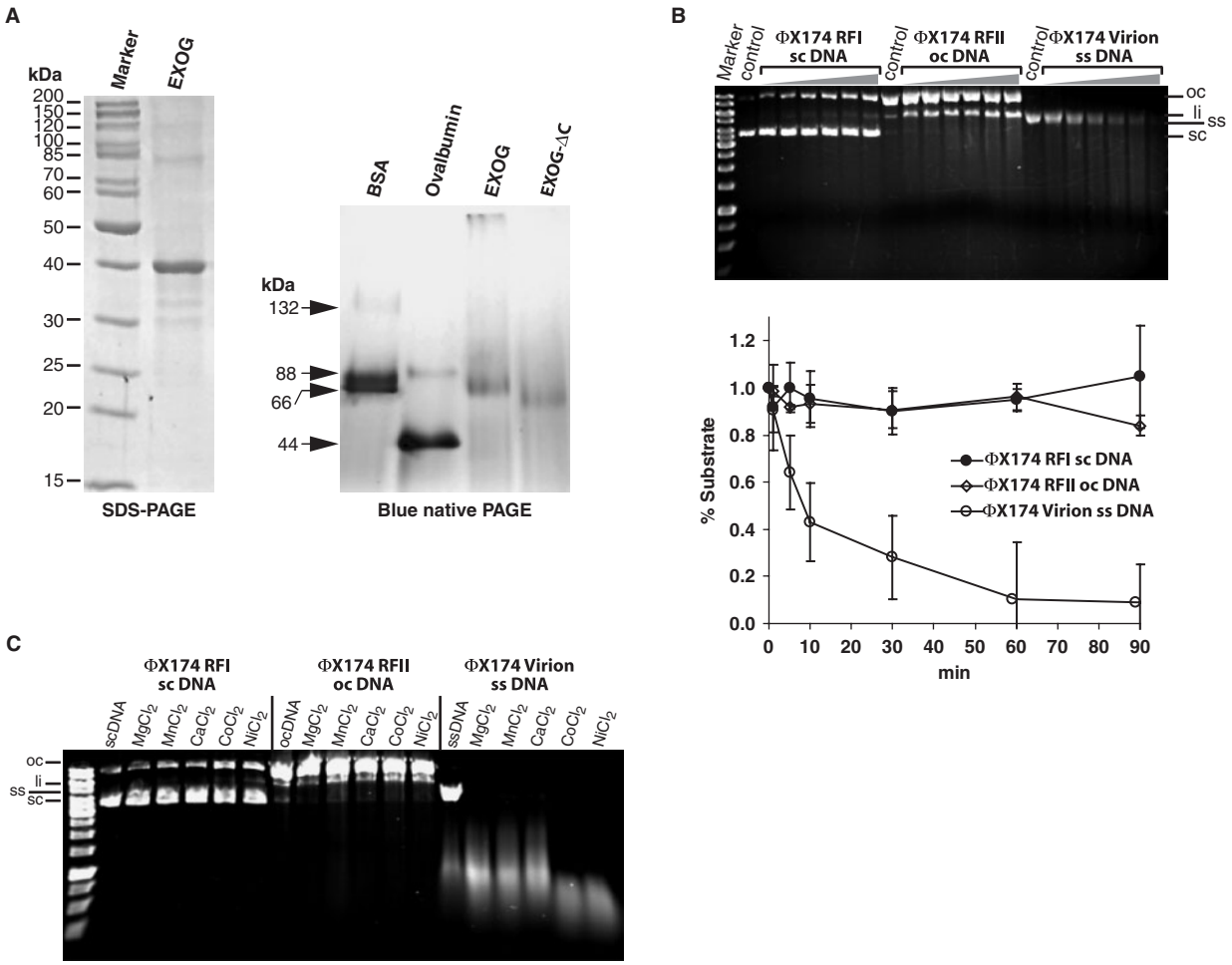

Figure 4. Recombinant EXOG is a homodimer. (**A**) Recombinant EXOG expressed in *E. coli* could be purified via Ni^{2+}-NTA affinity chromatography under denaturing conditions and was refolded by flash dilution into a renaturation buffer derived from the iFold-2 system. On SDS-PAGE, the protein (2.7 µg) runs with the expected size of 40 kDa (left panel). Blue Native PAGE reveals that full length EXOG (2.7 µg) and the EXOG-ΔC variant (2.7 µg) are homodimers in solution (right panel), as derived from a comparison with the migration of BSA (66 kDa) and ovalbumin (44 kDa) (5 µg each) on the same gel. (**B**) Quantitative analysis of the relative activity (decrease in relative amount (%) of substrate versus time) of recombinant EXOG towards single and double stranded DNA substrates (ΦX174 DNA), as derived from three independent cleavage experiments analyzed by agarose gel electrophoresis. (**C**) Influence of different divalent metal ions on the substrate specificity of EXOG. Single and double stranded DNA substrates (ΦX174 DNA) were incubated with EXOG for 10 min in a buffer consisting of 50 mM Tris pH 7.0, supplemented with 2.5 mM of the indicated divalent metal ions.

primary sequence of the protein and identified a hydrophobic N-terminal transmembrane segment (TMS, residues 16–38) folding into a putative transmembrane helix within the potential signal peptide (Figure 1A). To investigate the role of the putative TMS we deleted the region comprising amino acid residues 1–15 as well as the entire predicted signal sequence that includes the putative transmembrane helix (residues 1–41). Whereas the Δ1-15-EXOG-EGFP variant was still found localizing to mitochondria as analyzed by confocal laser scanning microscopy, Δ1-41-EXOG-EGFP was evenly distributed in the cytosol of transfected cells, demonstrating that the first 15 amino acid residues are not essential for mitochondrial localization of EXOG but that the region spanning amino acid residues 16–41 comprising the predicted helical TMS most likely is required for mitochondrial uptake of EXOG (Figure 3C).

Recombinant EXOG is a dimeric enzyme with preference for single stranded DNA

To further characterize the enzymatic properties of EXOG we expressed in *E. coli* a version devoid of the potential N-terminal signal sequence (residues 1–41) but instead fused to an N-terminal His-tag. Recombinant EXOG had to be renatured from inclusion bodies by flash dilution into a buffer derived from the iFold-2 system, and upon SDS-PAGE, EXOG migrated as a single band corresponding to its theoretical molecular mass of approximately 40 kDa with a purity of usually more than 95% (Figure 4A, left panel). The recombinant enzyme turned out to be a dimer in solution as analyzed by a discontinuous native polyacrylamide gel electrophoresis assay known as 'blue native PAGE' (Figure 4A, right panel). Importantly, recombinant EXOG from *E. coli* displayed the same preference for single stranded virion

Table 1. Biochemical characteristics of selected mitochondrial sugar-non-specifc nucleases from lower and higher eukaryotes

Name	[a]Nuc1p	[b,c]EndoG	[d]EXOG
Organism	*S. cerevisiae*	*B. taurus*	*H. sapiens*
Intracellular localization	IMM	IMS, IMM, MM	IMM
Catalytic motif	DRGH	DRGH	SRGH
Number of residues	329	299	368
Theoretical mass	37.2 kDa	32.2 kDa	41.2 kDa
Oligomeric structure	Homodimer	Homodimer	Homodimer
5′–3′ exonuclease activity	Yes	No	Yes
Type of DNA ends	5′-PO_4^-, 3′-OH	5′-PO_4^-, 3′-OH	5′-PO_4^-, 3′-OH
Me^{2+} ion requirement	$Co^{2+} \geq Mn^{2+} \geq Mg^{2+} > Zn^{2+} \geq Ca^{2+}$	$Co^{2+} > Mn^{2+} > Mg^{2+} \geq Ni^{2+} > Ca^{2+} \geq Zn^{2+} = Cu^{2+}$	$Co^{2+} = Ni^{2+} > Mn^{2+} \geq Mg^{2+} \geq Ca^{2+}$
Substrate specificity	ssDNA, RNA > dsDNA	ssDNA, dsDNA, RNA	ssDNA > dsDNA, RNA?[e]
pH-optimum	7.0–7.5	6.0 (5.0–8.0)	6.0 (ssDNA), 5.5 (dsDNA)

[a]Dake *et al.* (1988); [b]Low, 2003; [c]Schäfer *et al.*, 2004; [d]this work, see also Supplementary data; [e]on RNA, 5′–3′ exonuclease but no endonuclease activity could be detected (Meiss, unpublished); IMM, inner mitochondrial membrane; IMS, inter membrane space; MM, mitochondrial matrix.

DNA (7–10 × over open circular DNA and 14–20 × over supercoiled DNA) as the full length enzyme transiently expressed in mammalian cells (Figure 4B). However, upon prolonged incubation with recombinant EXOG, supercoiled and open circular DNA were also cleaved by the enzyme, resulting in the production of linear fragments of various sizes, as represented by a 'smear' upon agarose gel electrophoresis and ethidium bromide staining. The addition of non-ionic detergents such as Tween-20 to the renaturation and reaction buffer further enhanced the overall activity of refolded EXOG but did not change the preference of the enzyme for single stranded DNA (data not shown). Interestingly, supercoiled DNA is readily relaxed to the open circular form upon incubation with recombinant EXOG, similarly as seen with the immunoprecipitated enzyme preparation in Figure 1B, confirming a robust nicking activity displayed by EXOG (Figure 4B). As seen with EndoG, a variety of divalent metal ions can act as a cofactor for EXOG, but these different metal ions do neither influence the preference of EXOG for cleavage of single stranded DNA (Figure 4C), nor induce significant changes in the 5′–3′ exonuclease activity of EXOG (see Figure 6A). It should be noted here, that without addition of metal ions the EXOG preparation does not show nuclease activity (data not shown).

A detailed description of the biochemical properties of recombinant EXO and of two selected homologous enzymes, Nuc1p and EndoG, is compiled in Table 1 and Supplementary Figure S3.

Exchange of His140 from the catalytic SRGH-motif inactivates EXOG

The active site of sugar non-specific nucleases from various pro- and eukaryotes structurally is highly conserved (38,39). The availability of crystal structures from *Serratia* nuclease and NucA from *Anabaena* species (38,40,41) thus allowed us obtaining models of the active sites of EndoG and EXOG (Figure 5A). Since the amino acid composition of the catalytic motif of EXOG differs from that of most other mitochondrial sugar non-specific nucleases (SRGH- *versus* DRGH-motif) we produced by site-directed mutagenesis the single mutants S137D and H140A (Figure 5B) and measured their activity using single stranded virion DNA as substrate (Figure 5C and D). Prior to performing activity assays (see Materials and Methods section) the protein concentrations of the individual mutants were determined spectrophotometrically from the supernatant after renaturation by flash dilution and centrifugation as described under Materials and Methods, in order to account for possibly different levels of refolding of the mutant enzymes. As a result, reversion of Ser137 from the catalytic motif of EXOG to the more common aspartic acid residue did neither significantly change enzymatic activity nor substrate specificity of EXOG, suggesting that the serine residue is not responsible for the differences in enzymatic properties and the substrate specificity of EXOG compared to EndoG. In contrast, exchange of His140 to Ala abolished enzymatic activity. This is in line with our previous finding that the histidine residue from the catalytic DRGH-motif of related enzymes acts as a general base in the proposed mechanism of phosphodiester bond cleavage (31,39,42).

An SNP-related mutation inactivates EXOG

During our studies on EXOG we found an exonic SNP in the databases concerning exon 6 of the EXOG encoding gene that leads to variants of the enzyme with either a glycine or a valine residue at position 277 close to the predicted C-terminal coiled coil domain in the protein (Figure 1C). To investigate the effect of this SNP-related amino acid exchange on EXOG activity we produced by site directed mutagenesis the G277V variant. Intriguingly and unexpectedly, the mutation of Gly277 to Val had a similar effect on enzyme activity as the mutation of the conserved active site histidine residue His140 to Ala, indicating that the related SNP might play an important role in determining EXOG activity in humans (Figure 5C and D).

Deletion of the C-terminal domain inactivates EXOG

In contrast to previously characterized mammalian EndoG proteins EXOG-proteins posses a C-terminal domain that is predicted to fold into a coiled-coil structure (Figure 1A and Supplementary Figure S1). Deletion of

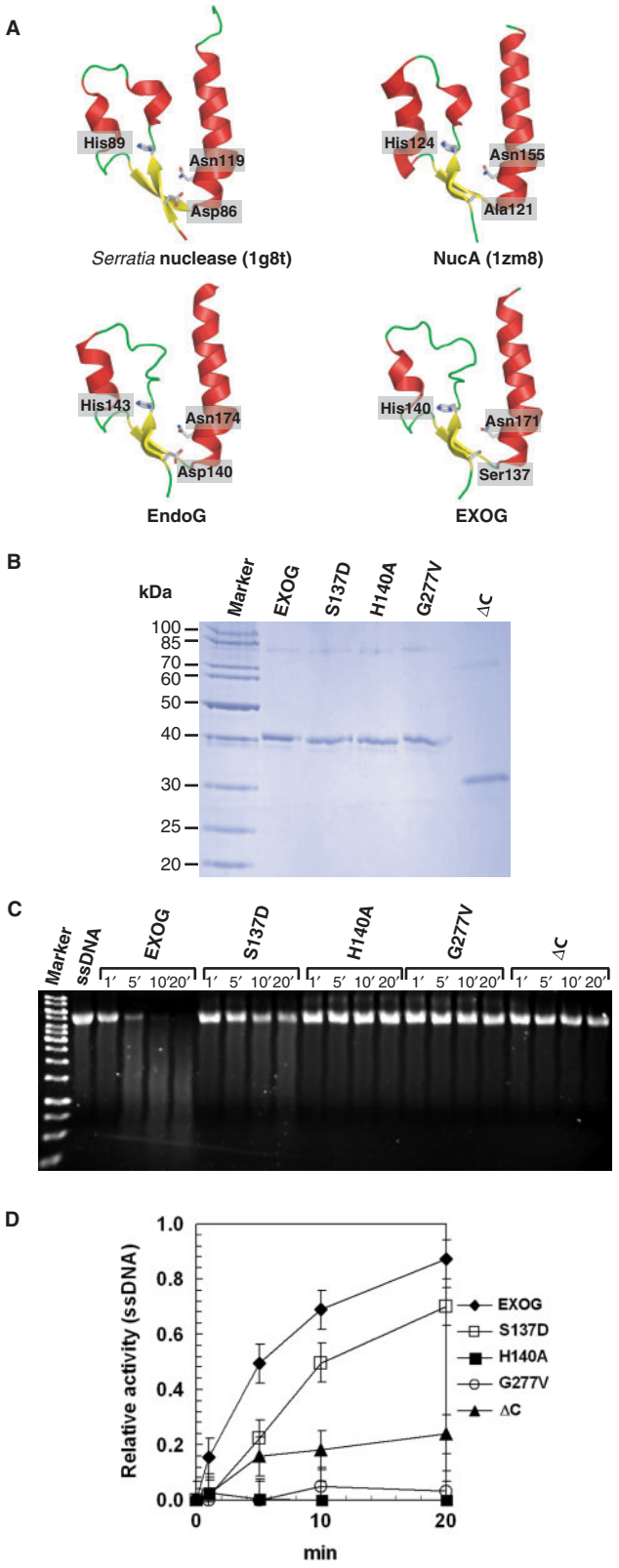

Figure 5. Mutational analysis of EXOG. EXOG has a serine residue in position 137 instead of an Asp as found in EndoG and most other sugar-non-specific nucleases. An exonic SNP found in the human *endonuclease G-like-1* gene leads to variants with either a Gly or a Val at position 277. In contrast to EndoG, EXOG has an additional C-terminal coiled-coiled domain. (**A**) Comparison of the active site structures of sugar non-specific nucleases. Based on the known crystal structures of homologous sugar non-specifc nucleases the active site structural motif of EXOG was modeled. (**B**) Purification and renaturation of single amino acid exchange and deletion variants of recombinant EXOG, as monitored by SDS-PAGE. (**C**) Relative activity of EXOG variants towards single stranded DNA as analyzed by agarose gel electrophoresis. Reversion of Ser137 to Asp only mildly lowers the activity of EXOG, whereas the substitution of the active site residue His140 to Ala and the SNP-related exchange of Gly277 to Val, as well as the deletion of the C-terminal domain inactivate the enzyme. (**D**) Plot of data as described under (C) derived from three independent cleavage experiments.

this domain leads to a pronounced reduction in EXOG activity, revealing that the presence and most likely the proper positioning of this domain of EXOG is crucial for its enzymatic activity (Figure 5C and D). Since Gly277 locates close to the C-terminal domain, it is tempting to speculate that the SNP-related G277V mutation might interfere with the correct positioning of this domain relative to the catalytic domain of EXOG, thereby inactivating the enzyme.

EXOG is an endo/exonuclease displaying 5′–3′ exonuclease activity

Since the single protein endo/exonuclease Nuc1p from yeast shows 5′–3′ exonuclease activity we next investigated the presence of such an activity in human EXOG by analyzing the cleavage of 12-mer and 27-mer oligonucleotides that were radioactively labeled at either the 5′- or the 3′-end by denaturing polyacrylamide gel electrophoresis as well as denaturing thin-layer ion exchange chromatography. Interestingly, EXOG shows a 5′–3′ exonuclease activity towards single and double stranded DNA (Figure 6 and Supplementary Figure S4), as demonstrated by the removal of the label from the 5′-labeled oligodeoxynucleotides by the enzyme. As seen from Figure 6A, on ssDNA the enzyme produces di- and mononucleotides, whereas on the dsDNA substrate dinucleotides were the predominant product. In these assays, we also used wild type EXOG and the active variant S137D as well as all other mutant forms of the enzyme (H140A, G277V and ΔC) with changes abolishing activity (Figure 6B and Supplementary Figure S4). The EXOG variants H140A, G277V and ΔC did not show the 5′–3′ exonuclease activity, indicating that the observed exonuclease activity does not result from a possible co-purified contamination. This result further suggests that endo- and exonucleolytic activity towards DNA is catalyzed by the same active site in the enzyme, since exchange of the catalytic histidine residue His140 abolishes both, endo- and exonuclease activity in EXOG.

When the 3′-labeled substrate was subjected to cleavage by EXOG only internal cleavage of the single stranded DNA was observed (Supplementary Figure S4), indicating that removal of the label from the 5′-end in addition to internal cleavage of a substrate indeed result from a combined endo/exonuclease activity in EXOG. EXOG did show little, if any, endonuclease activity on ribosomal RNA substrates in comparable experiments, however, exerted 5′–3′ exonuclease activity towards single stranded RNA (data not shown).

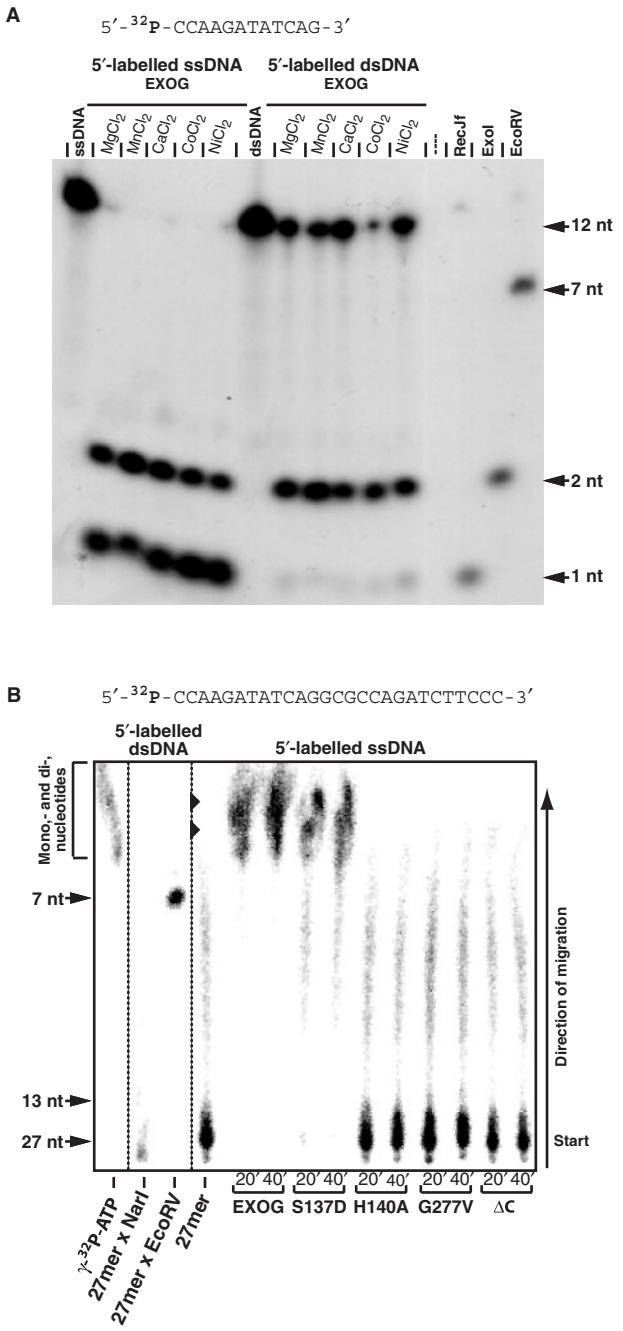

Figure 6. EXOG is an endo/exonuclease that exerts 5′–3′ exonuclease activity. (**A**) Exonuclease activity of EXOG on 5′-labeled single and double stranded DNA (5′-CCAAGATATCAG-3′) as revealed by production of di- and mononucleotides in the presence of different divalent metal ion cofactors. Shown is an autoradiogram after separation of cleavage products by 25% denaturing (7 M urea) polyacrylamide gel electrophoresis. Products from cleavage of the substrates with the REase EcoRV (7 nt) and the exonucleases $RecJ_f$ (5′–3′ exonuclease producing mononucleotides, 1 nt) and ExoI (3′–5′ exonuclease leaving a dinucleotide (2 nt) upon ultimate cut) were used as size markers. (**B**) EXOG variants H140A, G277V and ΔC do not show 5′–3′ exonuclease activity. Autoradiogram after separation by denaturing thin layer anion-exchange chromatography of products from the cleavage of single stranded DNA by EXOG. Products from cleavage of the corresponding double stranded substrate with the REases EcoRV (7 nt) and NarI (13 nt) as well as [γ^{32}P]-ATP were used as length markers. The migration of mono- and dinucleotides is indicated by arrowheads.

DISCUSSION

Nuc1p, also termed 'yeast EndoG', is a single mitochondrial sugar non-specific endo/exonuclease that regulates life and death in yeast (8,13). In *C. elegans* and mammals the Nuc1p homolgs CPS-6 and EndoG exert similar functions, yet the pathways leading to their activation are different (9,12,14). We find that rather than containing a single sugar non-specific nuclease, as found in lower eukaryotes, mitochondria of higher eukaryotes in addition to EndoG contain members of the paralogous EXOG-protein subfamily. Whereas mammalian EndoG is a pure endonuclease cleaving single and double stranded DNA and RNA with nearly identical rates, we find that human EXOG is a mitochondrial endo/exonuclease with nicking activity towards supercoiled DNA, a preference for single stranded DNA and 5′–3′ exonuclease activity. Such differences in enzymatic activities and substrate specificities suggest a subdivision of cellular functions between these two paralogous enzymes in higher eukaryotes. Its activities in principle endow EXOG with the ability to generate single stranded gaps in double stranded DNA required for DNA recombination and repair (7), pointing towards a role of EXOG in normal cell proliferation similarly as seen with yeast Nuc1p (8,10). Though such functions have been previously reported for EndoG (10), it seems more likely that this enzyme rather plays a major role in programmed cell death than DNA recombination and repair. Interestingly, several studies have previously described an enzymatic activity in mammalian mitochondria similar to yet clearly distinct from EndoG, whose enzymatic activities, e.g. preference for single stranded DNA, and whose biochemical properties, e.g. molecular weight, very much resemble those of EXOG proteins as described in this study (43,44). Whether these enzymatic activities correspond to EXOG currently is unknown and remains to be shown.

A combination of the results of mitochondrial subfractionation and electron microscopy experiments revealed that EXOG resides in the inner mitochondrial membrane. We assume that a predicted TMS, which very likely folds into a helix (TMH), serves to mediate association of EXOG with the inner mitochondrial membrane. Upon staurosporine induced apoptosis, EXOG remained clearly mitochondrial, whereas cytochrome *c* was increasingly released from mitochondria (Supplementary Figure S5).

The identification of EXOG as a novel mitochondrial endo/exonuclease provides an entirely new perspective for investigations on the role of mitochondrial nucleases during cell death and normal cell proliferation in eukaryotes. Our finding that EXOG and EndoG have complementary and partially overlapping enzymatic activities might explain why single knock-outs of EndoG in mice do not lead to an obvious phenotype, since EXOG could have simply stood in for at least some of the lost EndoG functions. Thus, it will be interesting to see the effects of double knock-out studies of EndoG and EXOG in mammals. Interestingly, we demonstrate that a single nucleotide polymorphism (SNP) found in exon 6 of the EXOG gene inactivates the enzyme. As it has been shown

that intronic SNPs in the EXOG gene are associated with type II diabetes (23) we hypothesize that this exonic SNP might also be associated with the development of this or other diseases, since it determines the availability of EXOG activity in humans. In conclusion, we propose integrating EXOG into future investigations on the cell death and cell proliferation scenario previously solely linked to EndoG, as our results establish the concept of a split mitochondrial endo/exonuclease function in higher eukaryotes.

SUPPLEMENTARY DATA

Supplementary Data are available at NAR Online.

ACKNOWLEDGEMENTS

We thank Jan Kosinski for critically reading the manuscript, Heike Büngen for technical assistance, Grzegorz Wilczynski and Adam Gorlewicz for advice and expertize in post embedding and electron microscopy, and Jacek Jaworski for the kind gift of pDsRed2-Mito. I.A.C. is recipient of a scholarship from SMM (Postgraduate School of Molecular Medicine) and has a young investigator award from FNP (Foundation for Polish Science). J.M.B. was supported by a grant from the NIH (1R33CA97899-01A from the NCI). I.C., B.M.B., and G.M. were supported by grant Pi 122/20-1 and the international research training group GRK 1384 from the DFG (German Science Foundation). Funding to pay the Open Access publication charges for this article was provided by DFG (German Science Foundation).

Conflict of interest statement. None declared.

REFERENCES

1. Low,R.L. (2003) Mitochondrial Endonuclease G function in apoptosis and mtDNA metabolism: a historical perspective. *Mitochondrion*, **2**, 225–236.
2. Garrido,C. and Kroemer,G. (2004) Life's smile, death's grin: vital functions of apoptosis-executing proteins. *Curr. Opin. Cell. Biol.*, **16**, 639–646.
3. Saelens,X., Festjens,N., Vande Walle,L., van Gurp,M., van Loo,G. and Vandenabeele,P. (2004) Toxic proteins released from mitochondria in cell death. *Oncogene*, **23**, 2861–2874.
4. Dake,E., Hofmann,T.J., McIntire,S., Hudson,A. and Zassenhaus,H.P. (1988) Purification and properties of the major nuclease from mitochondria of Saccharomyces cerevisiae. *J. Biol. Chem.*, **263**, 7691–7702.
5. Vincent,R.D., Hofmann,T.J. and Zassenhaus,H.P. (1988) Sequence and expression of NUC1, the gene encoding the mitochondrial nuclease in Saccharomyces cerevisiae. *Nucleic Acids Res.*, **16**, 3297–3312.
6. Parrish,J., Li,L., Klotz,K., Ledwich,D., Wang,X. and Xue,D. (2001) Mitochondrial endonuclease G is important for apoptosis in C. elegans. *Nature*, **412**, 90–94.
7. Zassenhaus,H.P. and Denniger,G. (1994) Analysis of the role of the NUC1 endo/exonuclease in yeast mitochondrial DNA recombination. *Curr. Genet.*, **25**, 142–149.
8. Buttner,S., Eisenberg,T., Carmona-Gutierrez,D., Ruli,D., Knauer,H., Ruckenstuhl,C., Sigrist,C., Wissing,S., Kollroser,M., Frohlich,K.U. *et al.* (2007) Endonuclease G regulates budding yeast life and death. *Mol. Cell*, **25**, 233–246.
9. Li,L.Y., Luo,X. and Wang,X. (2001) Endonuclease G is an apoptotic DNase when released from mitochondria. *Nature*, **412**, 95–99.
10. Huang,K.J., Ku,C.C. and Lehman,I.R. (2006) Endonuclease G: a role for the enzyme in recombination and cellular proliferation. *Proc. Natl Acad. Sci. USA*, **103**, 8995–9000.
11. Widlak,P. and Garrard,W.T. (2005) Discovery, regulation, and action of the major apoptotic nucleases DFF40/CAD and endonuclease G. *J. Cell Biochem.*, **94**, 1078–1087.
12. Arnoult,D., Gaume,B., Karbowski,M., Sharpe,J.C., Cecconi,F. and Youle,R.J. (2003) Mitochondrial release of AIF and EndoG requires caspase activation downstream of Bax/Bak-mediated permeabilization. *EMBO J.*, **22**, 4385–4399.
13. Burhans,W.C. and Weinberger,M. (2007) Yeast endonuclease G: complex matters of death, and of life. *Mol. Cell*, **25**, 323–325.
14. Wang,X., Yang,C., Chai,J., Shi,Y. and Xue,D. (2002) Mechanisms of AIF-mediated apoptotic DNA degradation in Caenorhabditis elegans. *Science*, **298**, 1587–1592.
15. Irvine,R.A., Adachi,N., Shibata,D.K., Cassell,G.D., Yu,K., Karanjawala,Z.E., Hsieh,C.L. and Lieber,M.R. (2005) Generation and characterization of endonuclease G null mice. *Mol. Cell Biol.*, **25**, 294–302.
16. David,K.K., Sasaki,M., Yu,S.W., Dawson,T.M. and Dawson,V.L. (2005) EndoG is dispensable in embryogenesis and apoptosis. *Cell Death Differ*.
17. Ekert,P.G. and Vaux,D.L. (2005) The mitochondrial death squad: hardened killers or innocent bystanders? *Curr. Opin. Cell Biol.*, **17**, 626–630.
18. Cote,J. and Ruiz-Carrillo,A. (1993) Primers for mitochondrial DNA replication generated by endonuclease G. *Science*, **261**, 765–769.
19. Cote,J., Renaud,J. and Ruiz-Carrillo,A. (1989) Recognition of (dG)n.(dC)n sequences by endonuclease G. Characterization of the calf thymus nuclease. *J. Biol. Chem.*, **264**, 3301–3310.
20. Ruiz-Carrillo,A. and Renaud,J. (1987) Endonuclease G: a (dG)n X (dC)n-specific DNase from higher eukaryotes. *EMBO J.*, **6**, 401–407.
21. Widlak,P., Li,L.Y., Wang,X. and Garrard,W.T. (2001) Action of recombinant human apoptotic endonuclease G on naked DNA and chromatin substrates: cooperation with exonuclease and DNase I. *J. Biol. Chem.*, **276**, 48404–48409.
22. Daigo,Y., Isomura,M., Nishiwaki,T., Tamari,M., Ishikawa,S., Kai,M., Murata,Y., Takeuchi,K., Yamane,Y., Hayashi,R. *et al.* (1999) Characterization of a 1200-kb genomic segment of chromosome 3p22-p21.3. *DNA Res.*, **6**, 37–44.
23. Moritani,M., Nomura,K., Tanahashi,T., Osabe,D., Fujita,Y., Shinohara,S., Yamaguchi,Y., Keshavarz,P., Kudo,E., Nakamura,N. *et al.* (2007) Genetic association of single nucleotide polymorphisms in endonuclease G-like 1 gene with type 2 diabetes in a Japanese population. *Diabetologia.*, **50**, 1218–1227.
24. Pei,J. and Grishin,N.V. (2007) PROMALS: towards accurate multiple sequence alignments of distantly related proteins. *Bioinformatics*, **23**, 802–808.
25. Abascal,F., Zardoya,R. and Posada,D. (2005) ProtTest: selection of best-fit models of protein evolution. *Bioinformatics*, **21**, 2104–2105.
26. Guindon,S., Lethiec,F., Duroux,P. and Gascuel,O. (2005) PHYML Online–a web server for fast maximum likelihood-based phylogenetic inference. *Nucleic Acids Res.*, **33**, W557–W559.
27. Whelan,S. and Goldman,N. (2001) A general empirical model of protein evolution derived from multiple protein families using a maximum-likelihood approach. *Mol. Biol. Evol.*, **18**, 691–699.
28. Anisimova,M. and Gascuel,O. (2006) Approximate likelihood-ratio test for branches: A fast, accurate, and powerful alternative. *Syst. Biol.*, **55**, 539–552.
29. Kurowski,M.A. and Bujnicki,J.M. (2003) GeneSilico protein structure prediction meta-server. *Nucleic Acids Res.*, **31**, 3305–3307.
30. Kabsch,W. and Sander,C. (1983) Dictionary of protein secondary structure: pattern recognition of hydrogen-bonded and geometrical features. *Biopolymers*, **22**, 2577–2637.
31. Schafer,P., Scholz,S.R., Gimadutdinow,O., Cymerman,I.A., Bujnicki,J.M., Ruiz-Carrillo,A., Pingoud,A. and Meiss,G. (2004) Structural and functional characterization of mitochondrial EndoG, a sugar non-specific nuclease which plays an important role during apoptosis. *J. Mol. Biol.*, **338**, 217–228.

32. Phend,K.D., Rustioni,A. and Weinberg,R.J. (1995) An osmium-free method of epon embedment that preserves both ultrastructure and antigenicity for post-embedding immunocytochemistry. *J. Histochem. Cytochem.*, **43**, 283–292.
33. Kirsch,R.D. and Joly,E. (1998) An improved PCR-mutagenesis strategy for two-site mutagenesis or sequence swapping between related genes. *Nucleic Acids Res.*, **26**, 1848–1850.
34. Kim,Y.S., Park,G.B., Choi,Y.M., Kwon,O.S., Song,H.K., Kang,J.S., Kim,Y.I., Lee,W.J. and Hur,D.Y. (2006) Ligation of centrocyte/centroblast marker 1 on Epstein-Barr virus–transformed B lymphocytes induces cell death in a reactive oxygen species–dependent manner. *Hum. Immunol.*, **67**, 795–807.
35. Niepmann,M. and Zheng,J. (2006) Discontinuous native protein gel electrophoresis. *Electrophoresis*, **27**, 3949–3951.
36. Altschul,S.F., Madden,T.L., Schaffer,A.A., Zhang,J., Zhang,Z., Miller,W. and Lipman,D.J. (1997) Gapped BLAST and PSI-BLAST: a new generation of protein database search programs. *Nucleic Acids Res.*, **25**, 3389–3402.
37. Schaffer,A.A., Aravind,L., Madden,T.L., Shavirin,S., Spouge,J.L., Wolf,Y.I., Koonin,E.V. and Altschul,S.F. (2001) Improving the accuracy of PSI-BLAST protein database searches with composition-based statistics and other refinements. *Nucleic Acids Res.*, **29**, 2994–3005.
38. Ghosh,M., Meiss,G., Pingoud,A., London,R.E. and Pedersen,L.C. (2005) Structural insights into the mechanism of nuclease A, a betabeta alpha metal nuclease from Anabaena. *J. Biol. Chem.*, **280**, 27990–27997.
39. Friedhoff,P., Franke,I., Meiss,G., Wende,W., Krause,K.L. and Pingoud,A. (1999) A similar active site for non-specific and specific endonucleases. *Nat. Struct. Biol.*, **6**, 112–113.
40. Lunin,V.Y., Levdikov,V.M., Shlyapnikov,S.V., Blagova,E.V., Lunin,V.V., Wilson,K.S. and Mikhailov,A.M. (1997) Three-dimensional structure of Serratia marcescens nuclease at 1.7 A resolution and mechanism of its action. *FEBS Lett.*, **412**, 217–222.
41. Yamashita,D., Miller,J.M., Jiang,H.Y., Minami,S.B. and Schacht,J. (2004) AIF and EndoG in noise-induced hearing loss. *Neuroreport*, **15**, 2719–2722.
42. Meiss,G., Gimadutdinow,O., Haberland,B. and Pingoud,A. (2000) Mechanism of DNA cleavage by the DNA/RNA-non-specific Anabaena sp. PCC 7120 endonuclease NucA and its inhibition by NuiA. *J. Mol. Biol.*, **297**, 521–534.
43. Davies,A.M., Hershman,S., Stabley,G.J., Hoek,J.B., Peterson,J. and Cahill,A. (2003) A Ca2+-induced mitochondrial permeability transition causes complete release of rat liver endonuclease G activity from its exclusive location within the mitochondrial intermembrane space. Identification of a novel endo-exonuclease activity residing within the mitochondrial matrix. *Nucleic Acids Res.*, **31**, 1364–1373.
44. Tomkinson,A.E. and Linn,S. (1986) Purification and properties of a single strand-specific endonuclease from mouse cell mitochondria. *Nucleic Acids Res.*, **14**, 9579–9593.